

The Macrocidins: Novel Cyclic Tetramic Acids with Herbicidal Activity Produced by *Phoma macrostoma*

Paul R. Graupner,*† Andy Carr,† Erin Clancy,† Jeffrey Gilbert,† Karen L. Bailey,‡ Jo-Anne Derby,‡ and B. Clifford Gerwick†

Natural Products Discovery, Dow AgroSciences, 9330 Zionsville Road, Indianapolis, Indiana 46268, and Agriculture & Agri-Food Canada, 107 Science Place, Saskatoon, Saskatchewan, Canada, S7N 0X2

Received April 30, 2003

Field isolates of *Phoma macrostoma* were obtained from diseased Canada thistle growing in several geographically diverse regions. Bleaching and chlorotic symptoms were present on the infected plants. The isolates grown in liquid culture were found to produce phytotoxic metabolites which also caused bleaching when applied foliarly to several broadleaf species. Bioassay-directed isolation led to the discovery of macrocidins A and B, the first representatives of a new family of cyclic tetramic acids. This new chemotype may offer significant potential as a template for herbicide design.

Plant pathogenic microbes have been the source of a wide range of unusual herbicidal metabolites. From pathogenic fungi alone are known novel alkaloids, terpenoids, peptides, macrolides, phenolics, and numerous other classes of compounds including compounds of mixed biogenesis.¹ It is generally acknowledged that these metabolites accelerate the virulence of many crop and weed pathogens.² Associated with these chemical compounds has been a range of unique modes of action.³ While none of these metabolites have demonstrated a sufficient level of activity or spectrum of activity to be commercialized, several have served as templates for the design of synthetic compounds. For example, moniliformin is produced by the pathogen *Fusarium moniliforme* and served as synthetic starting point for an extensive SAR at Ciba-Geigy.⁴ The compounds phaseolotoxin (a tripeptide containing the unusual amino acid octicidin) and coronatine from pathogenic *Pseudomonas* species have served as synthetic leads for efforts at Dow AgroSciences and elsewhere.⁵ Synthetic modification and simplification of herbicidal metabolites have typically resulted in loss of activity, such as reported in synthetic studies of herboxidiene.⁶ However, the synthesis of structurally related metabolites of eutypine, produced by the grape vine pathogen *Eutypa lata*, revealed at least one with greater phytotoxic activity than eutypine itself.⁷

We have studied the metabolites of several fungi at Dow AgroSciences, including species of the genus *Phoma*. There are more than 2000 species of the genus *Phoma* distributed throughout the world.⁸ Some species are known as plant pathogens, whereas others are saprophytes that colonize decaying plant tissues and live in soil. Several species also produce phytotoxic metabolites, such as phomalaidernone by *P. lingam*,⁹ nonenolides from *P. herbarum*,¹⁰ epoxydones from an unidentified *Phoma* sp.,¹¹ and putaminoxin from *P. putaminum*.¹² *Phoma macrostoma* Montagne [family: *Sphaeropsidaceae*] is a weak pathogen or wound parasite with a ubiquitous distribution. It causes chlorotic leaf spots and necrosis on woody and herbaceous plants,¹³ and black rot of artichoke leaves.¹⁴ There have been no reports on metabolites produced by *P. macrostoma*. This study investigated the phytotoxic metabolites produced by this fungal species in liquid culture.

Results and Discussion

Field isolates of *P. macrostoma* collected in Canada caused intense chlorosis and bleaching of emerging leaves of Canada thistle (*Cirsium arvense* L (scop)) when applied preemergently to soil (Figure 1). Culture extracts of these isolates caused intense bleaching of the new growth when applied postemergently to broadleaf plants. The bleaching resulted in slight growth inhibition after 4–6 days, but was lethal after 14 days in sunflowers. The plants appeared to develop almost normally for several days after treatment, although hypocotyls were frequently elongated and new leaves were completely white and reduced in size. Extracts from six strains of *P. macrostoma* (deposited at Agriculture & Agri-Food Canada, Saskatoon, Saskatchewan, as strains 94-44B, 94-359A, 95-268B, 94-26, 95-54A1, 95-54A2) produced identical symptoms in the bioassay and were examined by LC/MS linked to the bioassay. The extracts demonstrated activity in the same regions corresponding to two major factors of high polarity. The extracts from the mycelium and the freeze-dried broth produced indistinguishable effects and were pooled for all further studies.

The UV spectra of these compounds (15% aqueous CH₃CN, λ_{max} 202, 226, 245(sh), 284 nm) were unusual and helpful in guiding the purification process. LC/MS (-ESI) indicated a number of compounds with this UV spectrum, two of which were present in sufficient quantity to pursue identification. The main compounds were isolated by reversed-phase LC as described in the Experimental Section.

Structure Determination. The accurate mass of the major compound macrocidin A was 357.158 ($\text{C}_{20}\text{H}_{23}\text{NO}_5$ requires 357.1576). The proton NMR in methanol-*d*₄ had some features of note; all but two of the protons required for the molecular formula were apparent; two broad doublets which sharpened up at elevated temperature integrated for two protons each, suggesting a 1,4-disubstituted aromatic ring with some restricted rotation. Also present were a number of highly diastereotopic methylene signals, some at relatively high field, suggesting a conformationally constrained cyclic structure. Analysis of 2D COSY, TOCSY, HSQC, and HMBC experiments at 600 MHz and at 50 °C revealed two spin systems (Figure 2).

A small spin system with a methine at 4.13 ppm (*t*, $^3J_{\text{HH}} = 3.6$ Hz) was coupled to a methylene at 3.14 and 2.94 ppm

* Corresponding author. Tel: 1(317) 337 3496. Fax: 1(317) 337 3249. E-mail: prgraupner@dow.com.

† Dow AgroSciences.

‡ Agriculture and Agri-Food Canada.



Figure 1. Effect of soil treatment of *Phoma macrostoma* on Canada thistle plants. Left: control pots. Right: treated pots. Note intense bleaching of plants in the presence of fungus.

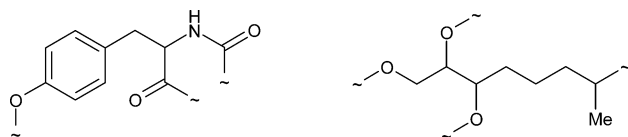


Figure 2. Spin systems for **1** from ^1H NMR.

($2 \times \text{dd}$; $^2J_{\text{HH}} = 14$ Hz; $^3J_{\text{HH}} = 3.6$ and 4.0 Hz). The similar magnitude of the vicinal coupling constants again implicated some conformational constraints for the molecule. Long-range correlations were seen in an HMBC (optimized for 8 Hz), which indicated an aromatic amino acid. Thus, the methylene signals correlated to two aromatic carbon atoms, and the methine to one, and also to an amide carbonyl at 177 ppm. The chemical shifts of the aromatic proton and carbon signals indicated an oxygen substitution *para* to the methylene, indicating tyrosine as an amino acid fragment.

The remaining signals in the proton spectrum were shown by COSY and TOCSY experiments to be part of a larger spin system. A methylene and two concurrent methines substituted with oxygen atoms were linked to three methylenes, with a methyl-substituted methine at the end (Figure 2). The coupling constant between the two oxygenated methine protons was small (2 Hz), although it was obvious from the TOCSY and HMBC experiments that they were connected. This was consistent with a *trans* epoxide connecting these two carbon atoms.

HMBC cross-peaks were noted between the oxygenated methylene and the aromatic carbon at 157 ppm, indicating connection to the tyrosine phenyl group through oxygen. The HMBC experiments also indicated that the methyl signal showed long-range cross-peaks to a signal at 193 ppm, and the tyrosine α proton to a carbon atom at 197 ppm, findings consistent with an acyl tetramic acid. In an experiment optimized for 4 Hz coupling, a minor cross-peak was noted from 12-H to the final carbon atom at 103 ppm, confirming the acyl tetramic acid. This accounts for the two exchangeable protons, confirming the presence of an epoxide between 16-C and 17-C .

Stereochemistry. Examination of 3D models of macrocidin A suggests that its rigid conformation would allow the determination of the relative stereochemistry of the

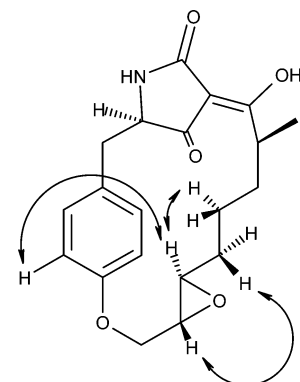


Figure 3. Representative NOE enhancements used to determine relative stereochemistry of macrocidin A.

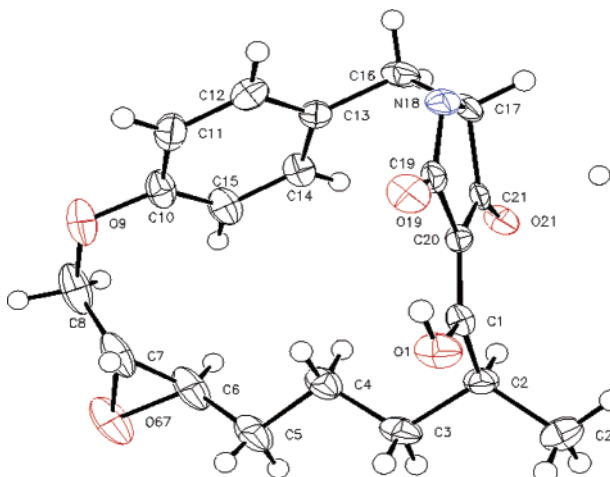
epoxide relative to the amino acid using a series of 2D ROESY and gNOE experiments.¹⁵ Irradiation of 17-H gave enhancements to 18-H , 16-H , and 14-H , whereas irradiation of 16-H —as well as enhancements to 13- , 14- , 17- , and 18-H —gave a very strong NOE to 3-H on the aromatic ring. These data were consistent only with the relative stereochemistry indicated in Figure 3; as for the opposite stereochemistry, it would be 17-H that would exhibit an NOE to the aromatic ring protons. It was not possible to find any NOE data to indicate the relative stereochemistry of the methyl group; however, the molecular models indicated that for one of the possible enantiomers the presence of this group would shepherd the carbon chain into a more highly ordered configuration than the other isomer. The measurement of large vicinal coupling constants between the protons in the chain suggested this to be the case. To show this—and confirm the relative stereochemistry of the epoxide—the structure was solved using a single-crystal X-ray diffraction (Figure 4). Unfortunately, the absolute stereochemistry remains undetermined due to paucity of sample.

Structure of Macrocidin B. The unusual UV spectrum of these molecules allowed the identification of a number of minor components in the crude extract. Only one other compound, however, was isolated in enough quantity to allow the structure to be determined with any degree of certainty due to its spectral similarity to macrocidin A. The

Table 1. NMR Assignments and HMBC Correlations for Macrocidins A and B

	macrocidin A ^a			macrocidin B ^b	
	¹³ C	¹ H (mult, J Hz)	HMBC ^d	¹³ C	¹ H (mult)
2	157.6 (s)			nd	
3	115.9 ^c (d)	6.84 (d, 8.7)	4, 18	114.7	6.83 (d 8.7)
4	132.6 (d)	7.05 (br d, 8.7)	3	131.2	7.01 (d, 8.7)
5	128.2 (s)		6	nd	
6	36.6 (t)	3.13 (dd, 13.8, 3.1) 2.94 (dd, 13.8, 4.0)	4, 6, 7	35.2	3.00 (dd, 14.1, 3.4) 2.82 (dd, 13.8, 4.0)
7	63.8 (d)	4.13 (t, 3.6)	6	nd	4.01 (t)
9	176.8 (s)		7	nd	
10	103.5 (s)		12 ^e	nd	
11	193.1 ^a (s)		13, 20	nd	
12	37.6 (d)	3.59 (m)	13, 20	60.5	3.46 (q, 6.9)
13	36.4 (t)	1.48 (ddd, 13.3, 11.2, 4.1) 1.38 (tt, 13.3, 4.1)	20	71.7	3.16 (t, 9.8)
14	25.4 (t)	1.16 (ddt, 13.3, 12.8, 4.1) 0.48 (ddt, 13.3, 12.8, 4.6)		31.4	1.01 (m) 0.62 (m)
15	34.3 (t)	1.92 (tt, 12.8, 3.6) 0.77 (dddd, 13.3, 10.2, 9.7, 5.1)		29.1	2.21 (m) 0.82 (m)
16	62.9 (d)	3.04 (ddd, 9.7, 3.1, 2.6)	15, 18	61.1	2.98 (m)
17	56.8 (d)	2.60 (dt, 8.7, 2.1)	18	55.1	2.58 (dt, 8.6m 2.1)
18	66.7 (t)	4.41 (dd, 12.8, 1.5) 3.96 (dd, 12.8, 8.7)	17	65.0	4.48 (12.9, 2.1) 3.94 (dd, 12.9, 8.1)
19	197.5 (s)		6	nd	
20	18.3 (q)	1.10 (d, 6.7)		15.0	1.06 (d, 6.9)

^a Spectra in CD₃OD at 25 °C; referenced to residual solvent at 3.31 ppm (¹H) and 49.5 (¹³C). A copy of the proton spectrum can be seen in the Supporting Information. ^b Spectra in DMSO at 50 °C, ¹³C data extracted from HSQC experiment (nd, signals not detected in these experiments). ^c Carbon signal broad. ^d Data from experiment optimized for 8 Hz unless noted. ^e Cross-peak in 4 Hz experiment only.

**Figure 4.** ORTEP diagram of crystal structure for macrocidin A.

mass of this factor (macrocidin B) was determined to be 16 amu greater than that of A, suggesting addition of a hydroxy group. The ¹H spectrum of macrocidin B (summarized in Table 1) differed from A in that there were only two aliphatic methylenes, and a new methine at 3.16 ppm, indicating hydroxy substitution on the backbone. COSY and TOCSY experiments indicated that the hydroxy group was situated on the carbon atom β to the methyl group. The coupling constant between 12-H and 13-H was small, suggesting that the protons were synclinal. From this observation, it may be possible to define the relative stereochemistry of the oxygen as well; however, no further evidence for this is available at present.

Dynamic NMR. This is the first example of a naturally occurring acyltetrameric acid containing a tyrosine amino acid. Other examples of acyltetrameric acids occurring within large rings have been reported (for example ikarugamycin¹⁶ and dihydromaltophilin¹⁷) though these tend to be derived from ornithine or other acyclic amino acids. The feature of tyrosine embedded in a macrocyclic molecule—while unusual—is not entirely unknown. The eurypamides are a group of related cyclic tripeptides in which two tyrosine amino acids are connected via an ether linkage between

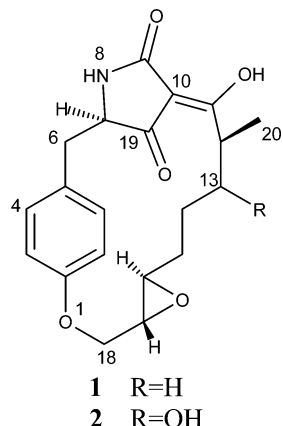
Table 2. Herbicidal Activity of Macrocidins Tested Postemergence on Greenhouse-Grown Weeds (rate in kg/hectare; see Experimental Section for species key)

compound	rate	HELAN	IPOHE	AVEFA	ECHCG
macrocidin A	3	50	65	0	0
macrocidin B	1	50	20	0	0

the two aromatic rings.¹⁸ The NMR of these peptides indicate that the aromatic ring of the tyrosine is conformationally restrained due to restricted rotation and resonates as four distinct multiplets. The line broadening in the macrocidins led us to reason that the rotation of the aromatic ring was somewhat restricted. Cooling the sample down in the NMR probe led to an increase in line broadening, with four distinct signals seen at -50 °C (data in Supporting Information).

Biological testing of the purified samples was completed following structure assignment. The tests were completed on greenhouse-grown plants. Each compound was applied postemergently to one pot containing four species. The results are shown in Table 2. After the 10-day grading period of this test, the activity of these compounds was significant on the broadleaf weeds but not apparent on the grass weeds. Although factor B could be tested only at a relatively low application rate of 1 kg/ha, significant chlorosis and growth inhibition was observed. The whole plant symptoms observed with the macrocidins are similar to those observed with sulcotriione and other inhibitors of hydroxyphenyl pyruvate dioxygenase (HPPD). However, an in vitro test of factors A and B against HPPD did not indicate any significant inhibition (data not shown). The mode of action remains unknown. The bleaching and stunting appeared primarily in the new growth of susceptible weeds, which suggested these compounds were phloem mobile. Indeed, the presence of an acidic tetrameric acid in a molecule of overall moderate lipophilicity (as judged by behavior on reversed-phase chromatography) is consistent with the physical properties known to impart phloem mobility.¹⁹ New chemotypes with phloem mobility and phytotoxicity are extremely rare,²⁰ and this new family of macrocyclic tetrameric acids may offer significant potential

as a template for herbicide design.



Experimental Section

General Experimental Procedures. All spectra were acquired on a Bruker DRX600 NMR spectrometer operating at 600.13 MHz (proton) and 150.92 MHz (carbon), with chemical shifts reported in ppm relative to internal solvent signals. For the structural identification, spectra were acquired in methanol-*d*₄ at 50 °C. LC/MS was performed on a Micromass Platform single-quadrupole mass spectrometer fitted with a Z-Spray LC/MS source and a Hewlett-Packard 1100 LC system. Accurate LC/MS experiments were conducted on a Micromass hybrid quadrupole-time-of-flight (Q-ToF) instrument equipped with a Hewlett-Packard 1100 LC system.

Fungal Isolation and Fermentation. Six strains of *P. macrostoma* were isolated from small chlorotic and necrotic lesions on leaf and stem tissues of Canada thistle plants collected from fields, pastures, and roadsides in three Canadian provinces between 1985 and 1997. Strains 94-44B, 94-359A, and 95-268B were from Saskatchewan, 94-26 from Ontario, and 95-54A1 and 95-54A2 from Nova Scotia. The strains were purified and verified for pathogenicity on Canada thistle (*Cirsium arvense*) using Koch's postulates.²¹

The spores and hyphae of each strain were stored by cryopreservation at -80 °C in vials of a 1:1 mixture of 10% skim milk (w/v) and 40% glycerol (v/v) at Agriculture & Agri-Food Canada, Saskatoon. Strains were revived by thawing a vial at room temperature and aseptically spreading the contents equally over 3–15 cm diameter Petri plates containing Difco potato dextrose agar (prepared according to manufacturer's directions) augmented with 3 mL of 85% lactic acid. The inoculated plates were incubated at ambient room temperature with natural light for 14 days.

For metabolite production, 5–6 mm diameter agar plugs from actively growing cultures were used to inoculate 12–500 mL flasks each containing 125 mL of Difco potato dextrose broth. Flasks were incubated in the dark at 15 °C for 4 weeks on a New Brunswick Scientific G-53 shaker rotating at 150 rpm. The contents of the flasks were pooled, vacuum filtered through two layers of cheesecloth, frozen, and freeze-dried prior to phytotoxin extraction.

Identification of Isolates as *Phoma macrostoma*. The six fungal strains used in this study were identified by the Centraalbureau voor Schimmelcultures, Utrecht, The Netherlands, as *P. macrostoma* var. *macrostoma* by using morphological and cultural characteristics on standardized media and environmental conditions *in vitro* as described by de Gruyter et al.²² These strains produced dark pycnidia with relatively wide ostioles which released salmon-colored conidial exudate containing 1–3-celled conidia. The var. *macrostoma* produces a dull red-violet pigment in the hyphae, as was characteristic with these strains. The var. *incolorata* is distinguished from var. *macrostoma* by the absence of the colored pigmentation in the hyphae.

Screening. Samples of mycelium extract (MeOH) and lyophilized broth from each isolate were dissolved in 100 μL

of 50% methanol containing 0.05% X-77 surfactant and sprayed using a fine misting nozzle onto one or more of the following plants at the seedling stage: sunflower (*Helianthus annuus*, *HELAN*), giant foxtail (*Setaria faberii*, *SETFA*), ivy leaf morning glory (*Ipomoea hederacea*, *IPOHE*), wild oat (*Avena fatua*, *AVEFA*), or barnyard grass (*Echinochloa crus-galli*, *ECHCG*). The plants were grown under greenhouse conditions. After 7–14 days plant injury was visually estimated as percent growth reduction by comparison to untreated controls, where 100% represents complete plant death and 0% represents no effect. Chromatographic fractions and isolated pure compounds were tested in a similar manner.

Isolation of Macrocidins A and B. The crude extracts (11 g after freeze-drying) were fractionated in 1 g aliquots by preparative HPLC (YMC ODS-AQ 50 mm × 25 cm; particle size, 10 μm) with a gradient of 10% acetonitrile to 50% acetonitrile in 10 mM ammonium acetate. Each fraction was bioassayed as described. Further fractionation of the later-eluting fractions that demonstrated biological activity was performed on an analytical scale using these same conditions, yielding macrocidin A (**1**, 3.5 mg). Repetitive isocratic chromatography of the earlier active fractions on a YMC ODS-AQ column (4.6 mm × 25 cm; particle size, 5 μm) using 6% acetonitrile in 10 mM ammonium acetate yielded macrocidin B (**2**, 1.2 mg).

Macrocidin A: pale beige solid; UV and NMR, see text and Table 1; $[\alpha]^{25}_D +45^\circ$ (*c* 0.35, MeOH); IR (NaCl) 3306 (br), 2966, 2934, 2861, 1711, 1662, 1611, 1510 cm^{-1} .

Macrocidin B: pale beige solid; NMR, see Table 1.

Acknowledgment. The authors would like to thank Phil Fanwick (Purdue University) for the solution of the crystal structure.

Supporting Information Available: A copy of the ¹H spectrum and dynamic spectra of macrocidin A—as well as detailed tables of the crystal structure—are available. This material is available free of charge via the Internet at <http://pubs.acs.org>.

References and Notes

- (1) Strobel, G.; Kenfield, D.; Bunkers, G.; Sugawara, F.; Clardy, J. *Experientia* **1991**, *47*, 819–826.
- (2) Gross, D. C. *Annu. Rev. Phytopathol.* **1991**, *29*, 247–278.
- (3) (a) Duke, S. O. *Rev. Weed Sci.* **1986**, *2*, 15–44. (b) Duke, S. O.; Dayan, F. E.; Romagni, J. G.; Rimando, A. M. *Weed Res.* **2000**, *40*, 99–111.
- (4) Pachlatko, J. P. *Chimia* **1998**, *52*, 29–47.
- (5) (a) Haider, G.; Von Schrader, T.; Fusslein, M.; Blechert, S.; Kutchan, T. M. *Biol. Chem.* **2000**, *381*, 741–748. (b) Schueler, G.; Boland, W.; Lauchli, R. *PCT Int. Appl.* WO 0255480, 2002.
- (6) Isaac, B. G.; Ayer, S. W.; Elliott, R. C.; Stonard, R. J. *J. Org. Chem.* **1992**, *57*, 7220–7226.
- (7) Smith, L. R.; Mahoney, N.; Molyneux, R. J. *J. Nat. Prod.* **2003**, *66*, 169–176.
- (8) Leath, K. T. *Methods for Research on Soilborne Phytopathogenic Fungi*; Singleton, L. L., Mihail, J. D., Rush, C. M., Eds.; APS Press: St. Paul, MN, 1992; pp 142–144.
- (9) Pedras, S. M.; Erosa-Lopez, C. C.; Quail, J. W.; Taylor, J. L. *Bioorg. Med. Chem. Lett.* **1999**, *9*, 3291–3294.
- (10) Rivero-Cruz, J. F.; García-Aguirre, G.; Cerdá-García-Rojas, C. M.; Mata, R. *Tetrahedron* **2000**, *56*, 5337–5344.
- (11) Venkatasubbaiah, P.; Chilton, W. S. *J. Nat. Prod.* **1992**, *55*, 639–643.
- (12) Evidente, A.; Lanzetta, R.; Capasso, R.; Andolfi, A.; Bottalico, A.; Vurro, M.; Zonno, M. C. *Phytochemistry* **1995**, *40*, 1637–1641.
- (13) Boerema, G. H.; Dorenbosch, M. M. J. *Persoonia* **1970**, *6*, 49–58.
- (14) Kubota, M.; Abiko, K. *J. Gen. Plant Path.* **2002**, *68*, 208.
- (15) Stott, K.; Keeler, J.; Van, Q. N.; Shaka, A. J. *J. Magn. Reson.* **1997**, *125*, 302–324.
- (16) Ito, S.; Hirata, Y. *Bull. Chem. Soc. Jpn.* **1977**, *50*, 1830.
- (17) Graupner, P. R.; Snipes, C. E.; Thornburgh, S.; Mathieson, J. T.; Chapin, E. L.; Kemmitt, G.; Brown, J. M. *J. Antibiot.* **1997**, *50*, 1014.
- (18) Rami Reddy, M. V.; Harper, M. K.; Faulkner, D. J. *Tetrahedron* **1998**, *54*, 10649–10656.
- (19) (a) Kleier, D. A. *Plant Physiol.* **1988**, *86*, 803–810. (b) Bromilow, R. H.; Chamberlain, K.; Evans, A. A. *Weed Sci.* **1990**, *38*, 305–314.
- (20) Gerwick, B. C.; Graupner, P. R.; Gray, J. A.; Peacock, C. L.; Hahn, D. R.; Chapin, E. L.; Schmitzer, P. R. *International Weed Control Congress*; Foz Do Iguaçu, Brazil, 2000.
- (21) Agrios, G. N. *Plant Pathology*, 2nd ed.; Academic Press: New York, 1978; pp 26–27.
- (22) Gruyter, J. de; Boerema, G. H.; Van der AA, H. A. *Persoonia* **2002**, *18*, 1–53.